Radiation Damage Study in
Advanced Nuclear Reactor Structural Materials

Ji-JUNG Kai
Professor and Director
Center for Energy and Environmental Research
Department of Engineering and System Science
National Tsing Hua University
Hsinchu, TAIWAN 30013 ROC

Present in "the Spent Nuclear Fuel Management Strategy Symposium",
INER, Lungtang, December 16-17, 2009

國立清華大學能源與環境研究中心
Center for Energy and Environmental Research

Radiation Effects

- The macroscopic, observable, and often technologically crucial results of exposure of solids to energetic particles are collectively known as "radiation effects".

Radiation Damage

The primary, microscopic events that precede the appearance of gross changes in the solids.

Radiation Damage:

- Radiation: energetic particles
- interstitials
- vacancies

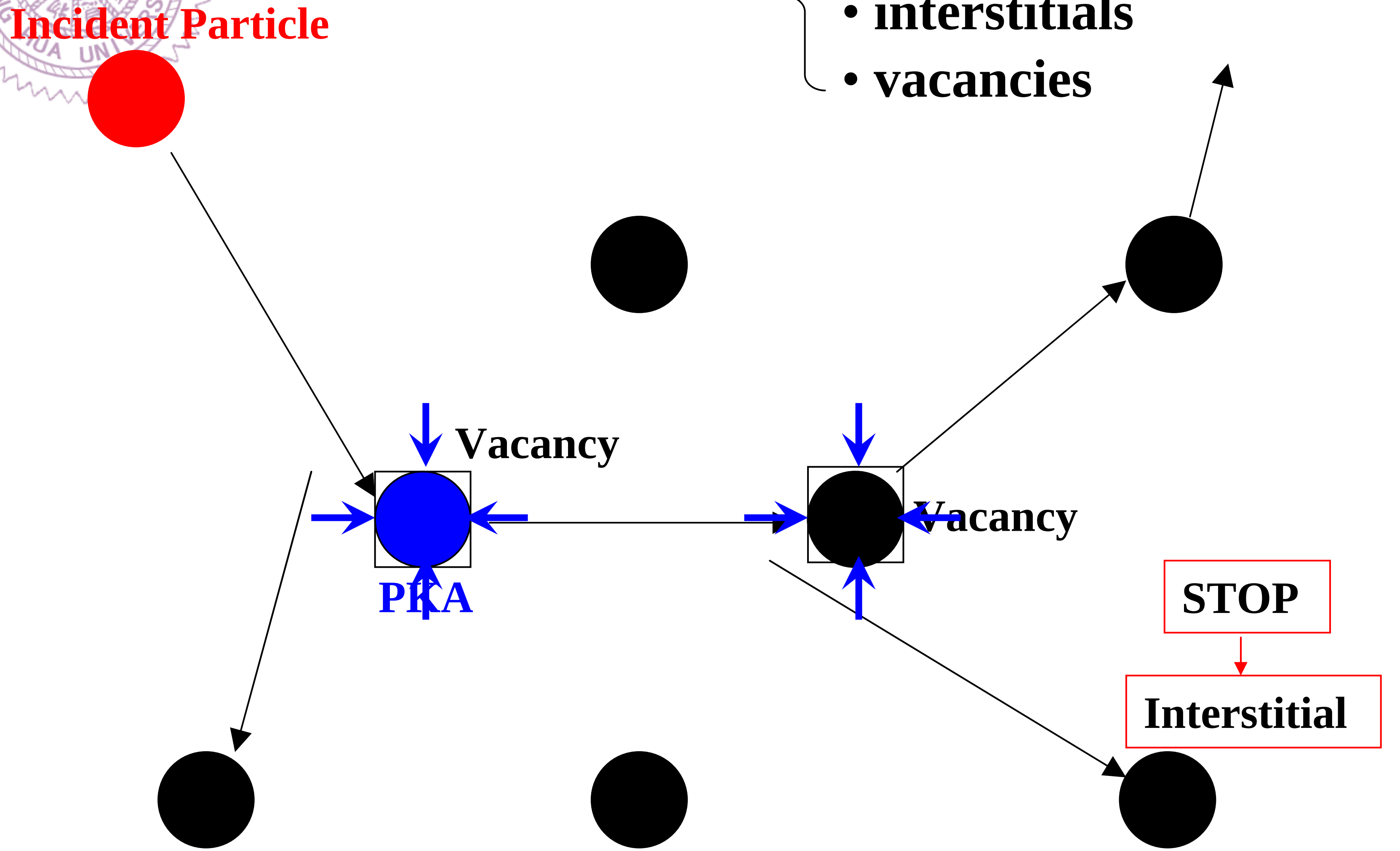

Time Scale

~~~~~~~~~~~~~~~

◆Energetic particles (Bombarding particles (E)):

•Neutron (fission: 1~2MeV ; fusion: 14MeV)

•Charge particles (fission fragments, (fission))

(P$^+$, D$^+$, T$^+$, He^{++},…..(fusion))

(other ions , accelerators)

<10^{-11}sec

•Electrons (accelerator , HVEM)

•Photons (γ -ray , X-ray)

◆ Interactomic potentials: { screened , partially screened , un-screened ….}

◆ Primary Knock-on Atoms: PKAs

PKA energy loss ;$(\partial E / \partial x)_n$ (displacement) , $(\partial E / \partial x)_e$ (heat)

~~~~~~~

◆ Secondary Knock-on Atoms (E") , cascades , spikes , ...

<seconds

◆ Migration to sinks : Recombination , defect clusters , microstructure changes

~~~~~~~~~~~~~~~

Hours, days, months

◆ Mechanical Property changes
Physical Property changes
Chemical property changes

} strength , fatigue , ductility , creep . swelling , electrical resist , corrosion , scc , ...
~~~~~~~~~~~~~~~

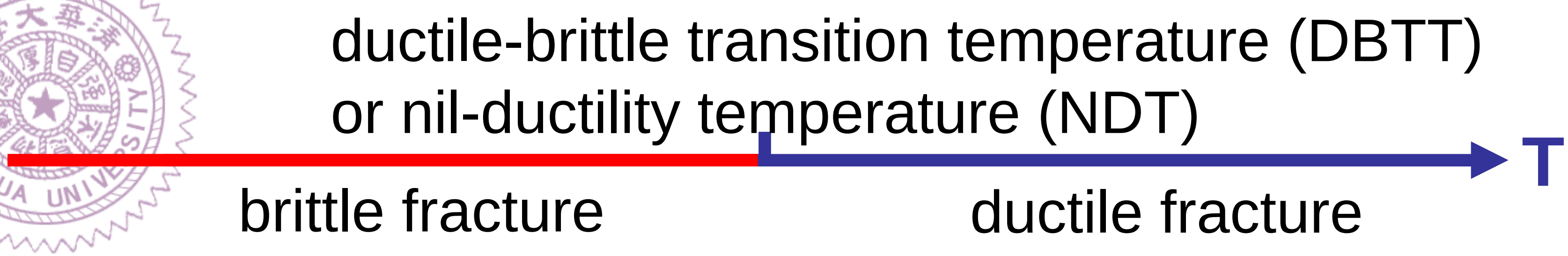

The nil-ductility temperature increases dramatically with neutron exposure.

Four broad categories of mechanical behavior are pertinent to reactor performance:

1. Radiation hardening
2. Embrittlement and fracture
3. Swelling
4. Irradiation creep

Radiation hardening means the increase in the yield stress and the ultimate tensile stress as a function of fast-neutron fluence and temperature. However, the strength of fuel-element cladding is most accurately represented by creep, since the internal loading on the cladding never reaches the yield stress.

Embrittlement of a metal is measured by the amount of plastic or creep deformation that occurs before fracture. Fast-neutron irradiation invariably renders a metal less ductile than the unirradiated materials.

Theories of Radiation Hardening

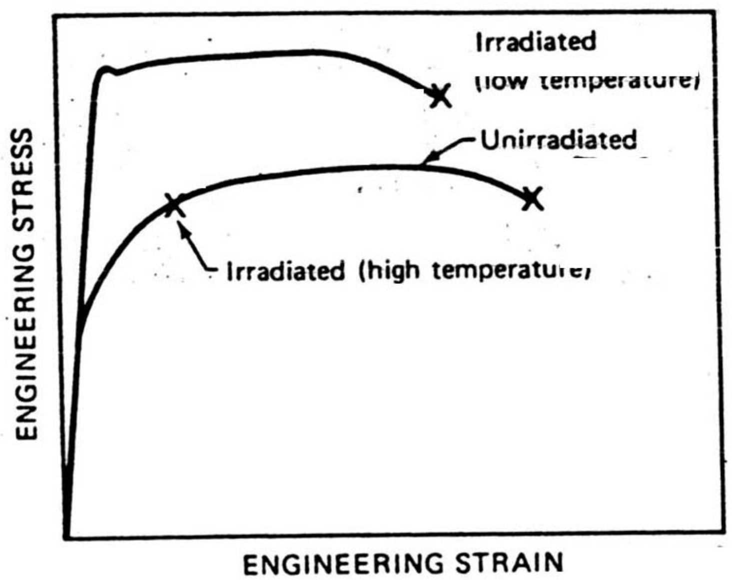

(a)

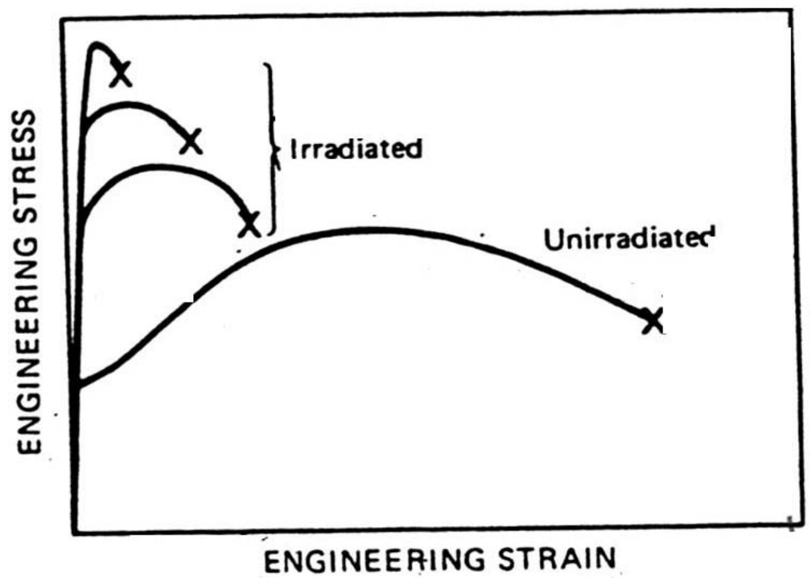

(b)

▪Radiation Hardening is attributed to various defects:

1. point defects (vacancies & interstitials)
2. impurity atom (transmutation products)
3. small vacancy clusters (depleted zone)
4. dislocation loops (v-type and i-type)
5. dislocation lines (loop increases up to large enough)
6. cavities (voids and helium bubbles)
7. precipitate (in steels, intermetallic phase or carbides)

The items from 3 to 7 are more important.

*point defects and impurity atoms are believed to contribute negligible to hardening compares to the defect of the large defect clusters.

§18.6 Hardening by Impenetrable Obstackes
—Precipitates and Voids

➢ A dislocation line moves through a field of impenetrable obstacles by bowing around them.

⇒precipitation hardening

➢ Coherent precipitates :

A dislocation “feels” the presence of such a particles via the stress field before actual contact is made.

➢ Incoherent precipitates:

The dislocation must physically contact the particle before the interaction force is appreciable.

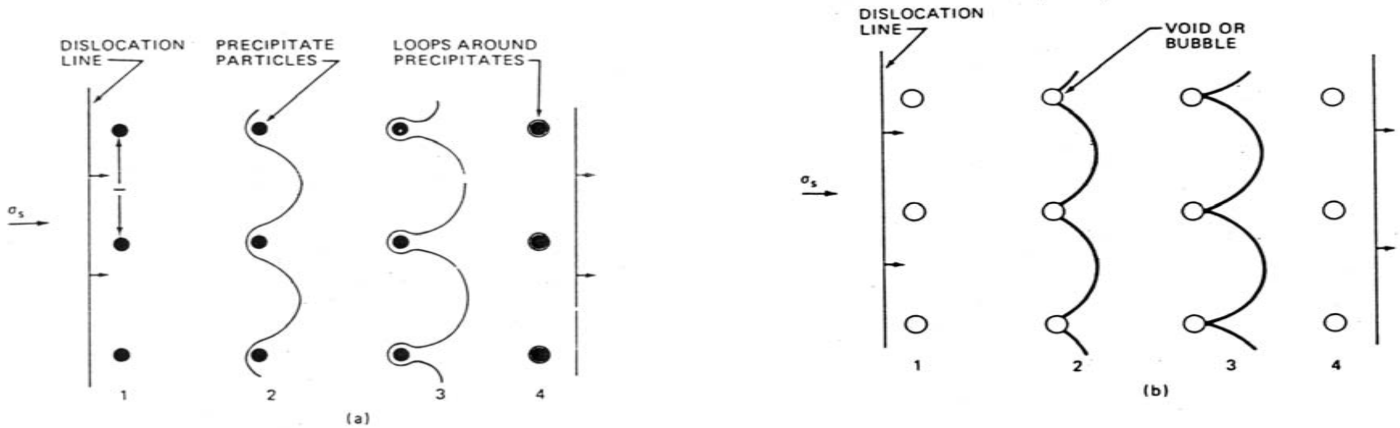

➢The dislocation motion is the same manner as a Frank-Reed dislocation source operates.

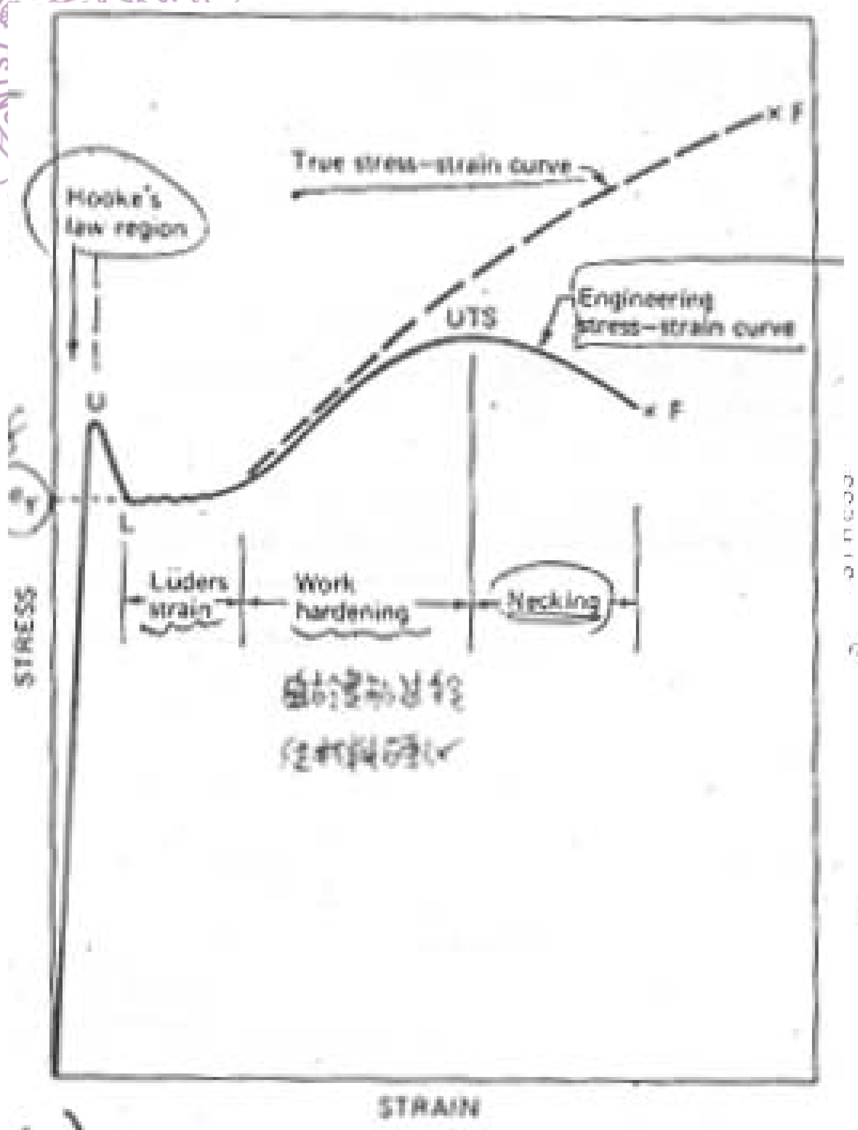

Fig. 18.10 Stress–strain curve for ferritic steel.

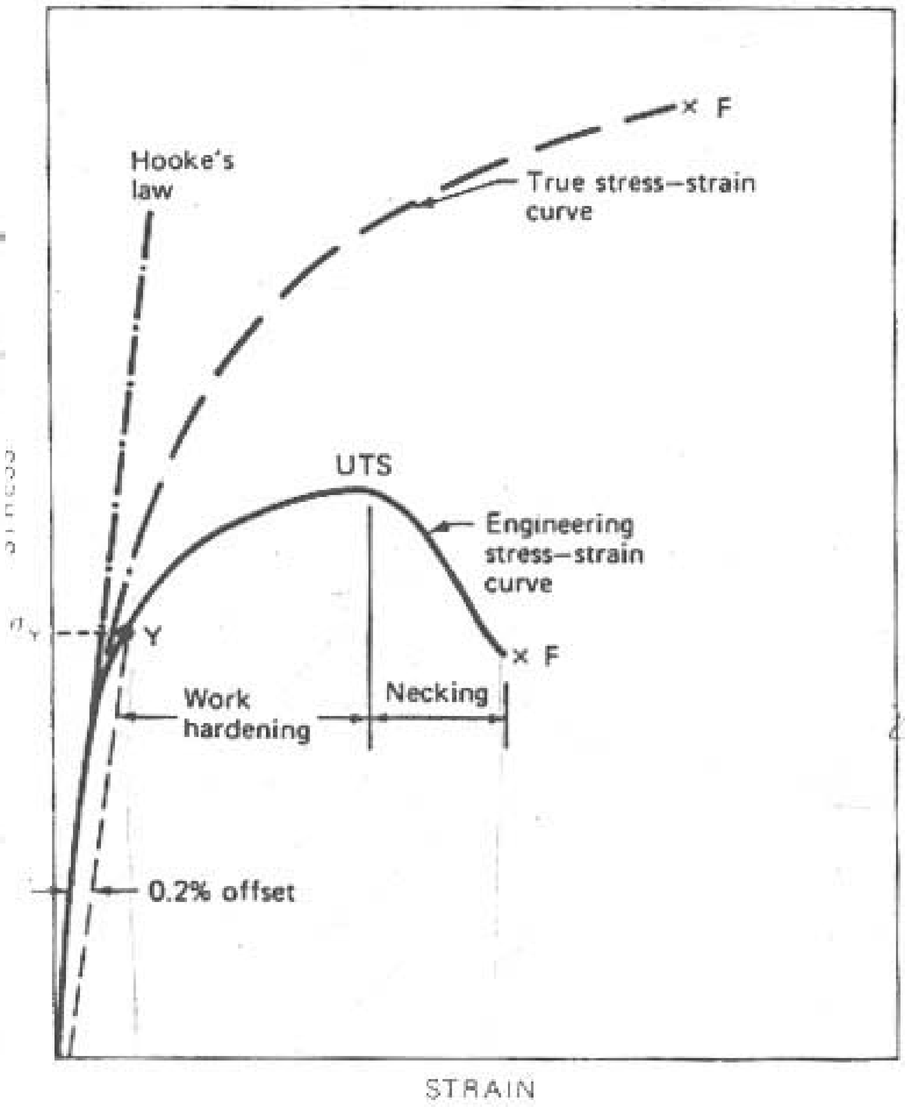

Fig. 18.11 Stress–strain curve for austenitic steel.

Charpy V-notch test:

Specimen size and shape:

$1 \times 1 \times 6 cm^3$

Initial hammer height h_1

=325Joul impact energy

The different between the initial and final heights of the hammer (h_1-h_2) give the energy absorbed by the specimen in the fracture process

BDTT: Ductile-Brittle transition temperatur

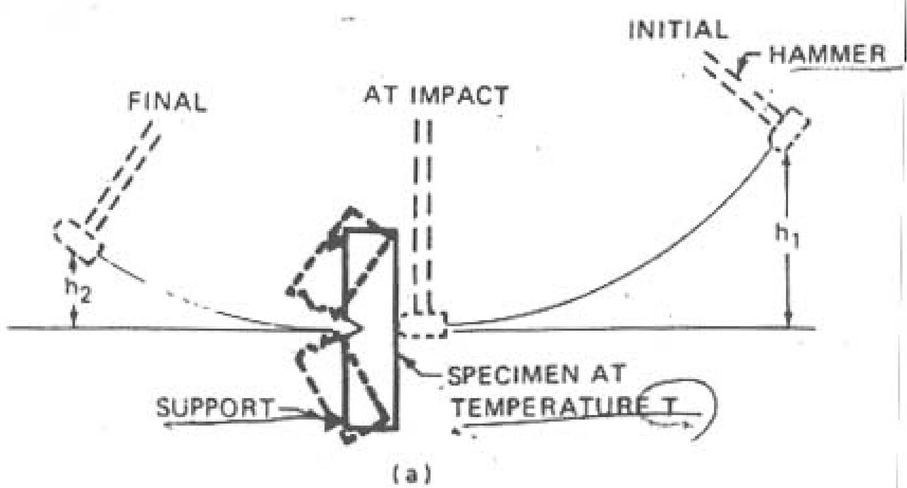

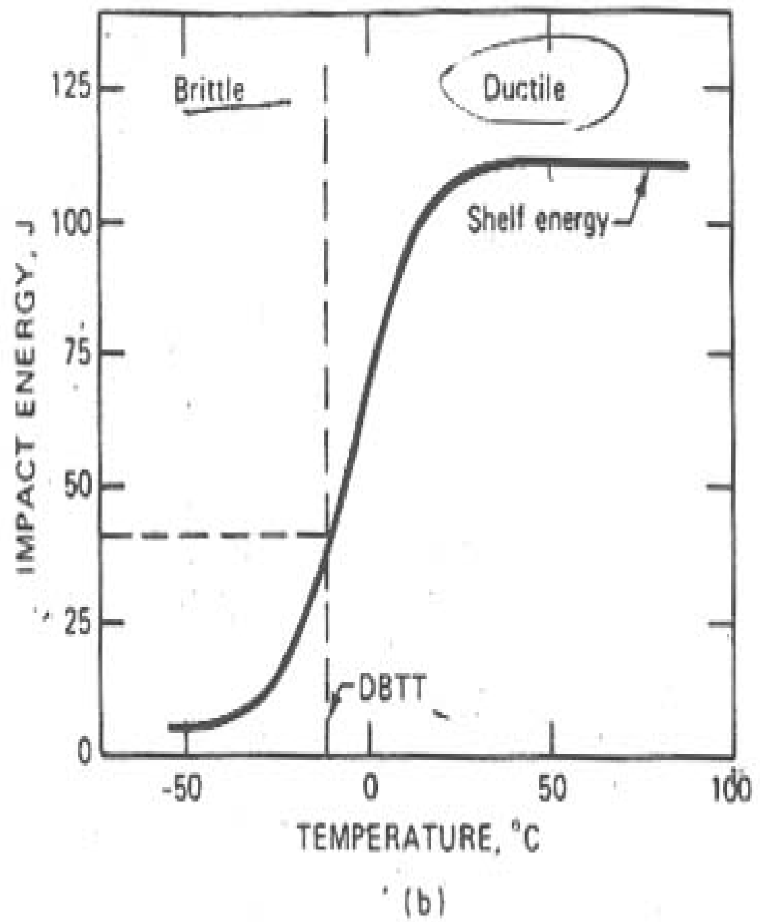

Fig. 18.13 The Charpy V-notch test. (a) Test setup. (b) Variation of absorbed energy with temperature.

核融合簡介

$D + T \rightarrow {}^{4}He$ (3.5 MeV) + n (14.1 MeV)

Tokamak 結構

示意圖

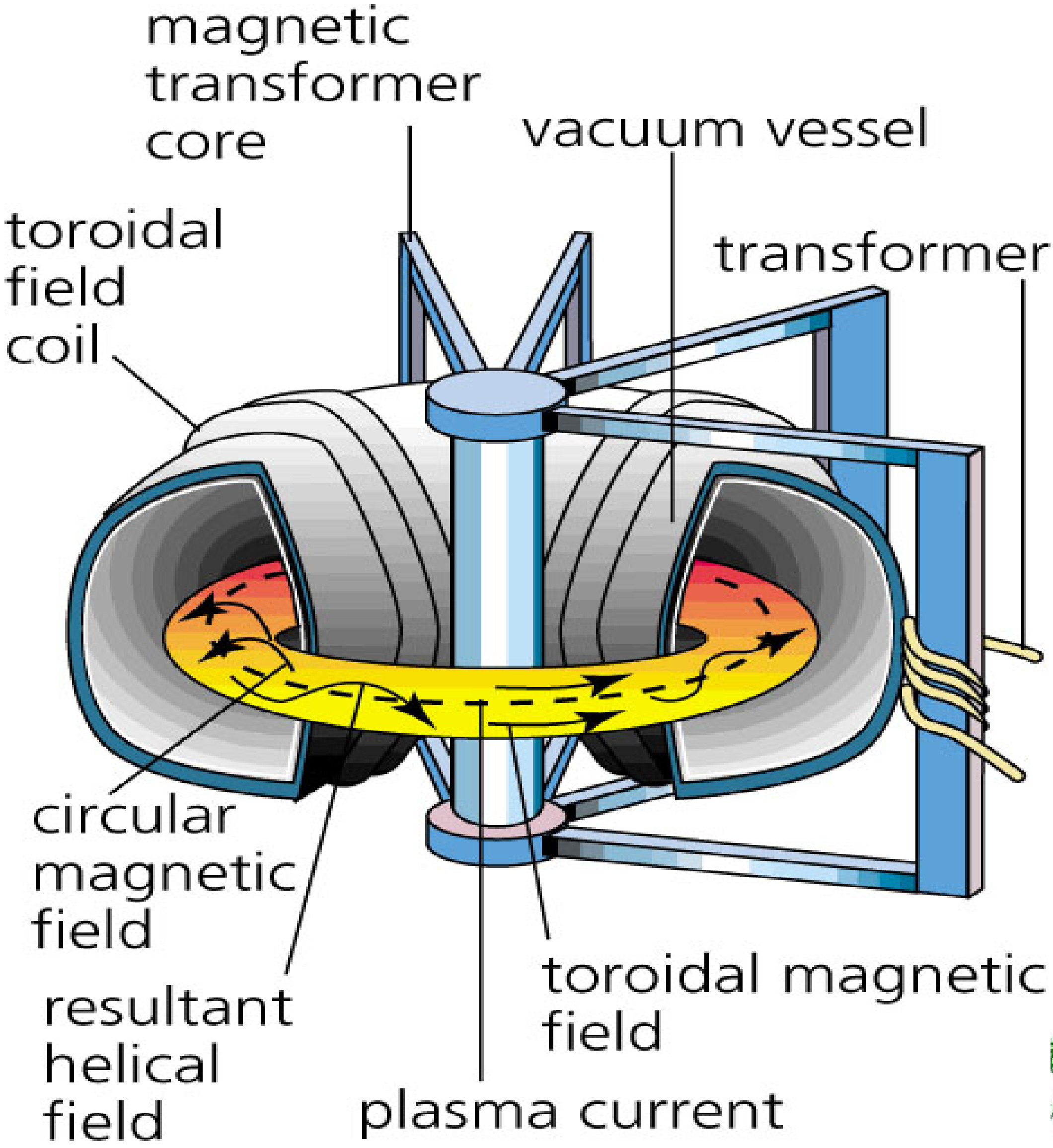

- 碳化矽複合材應用在Tokamak結構的First wall、blanket

- 右圖為國際熱核融合實驗爐ITER的概念設計圖，預計在2010年完成

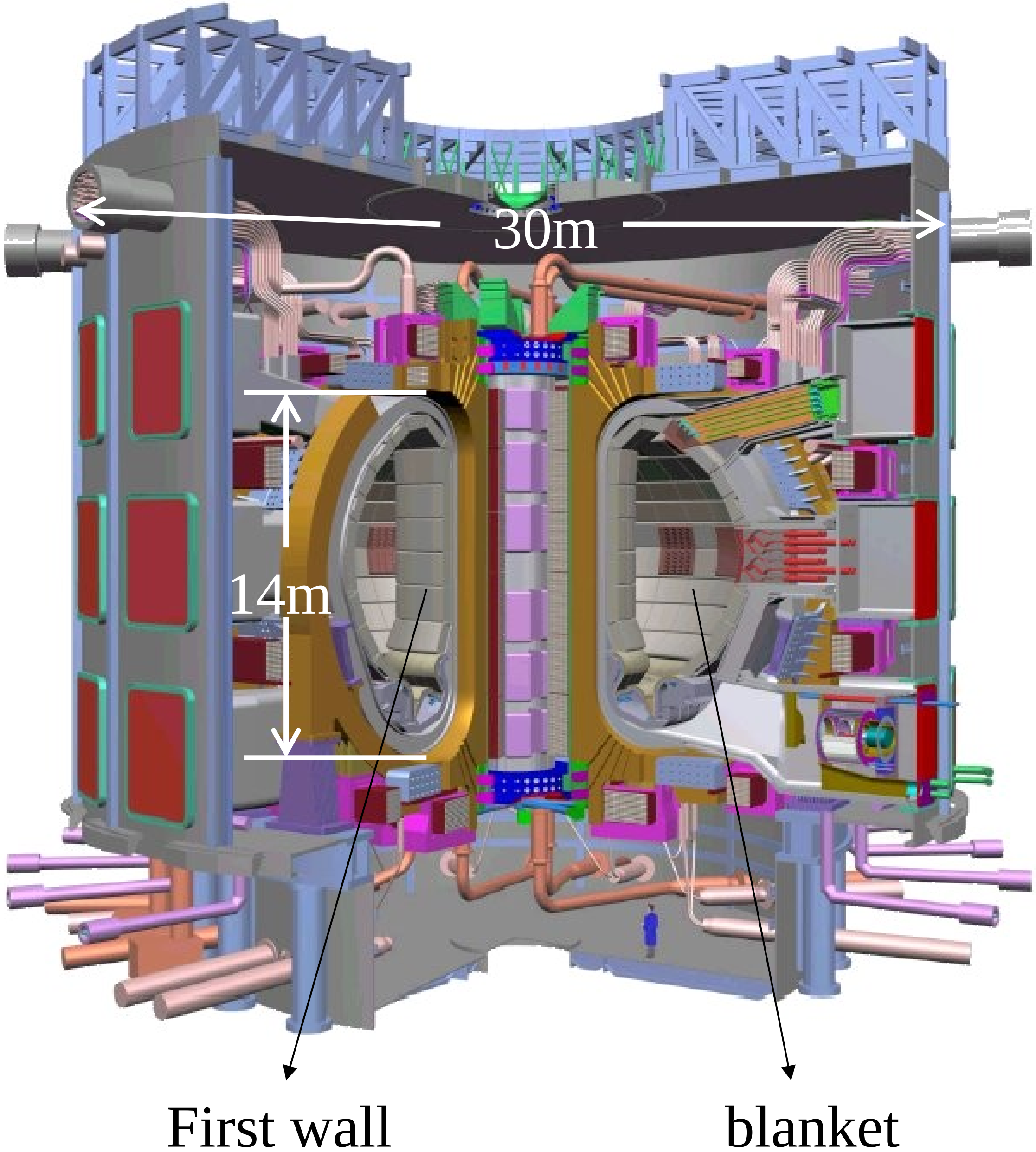

http://www-fusion-magnetique.cea.fr/iter/iter_coupe01.jpg

國立清華大學能源與環境研究中心
Center for Energy and Environmental Research

研究動機～結構材料所面臨的問題

1.高能中子造成材料輻射損傷(dpa)
2.(n，He)、(n，H)核轉化效應(appm)

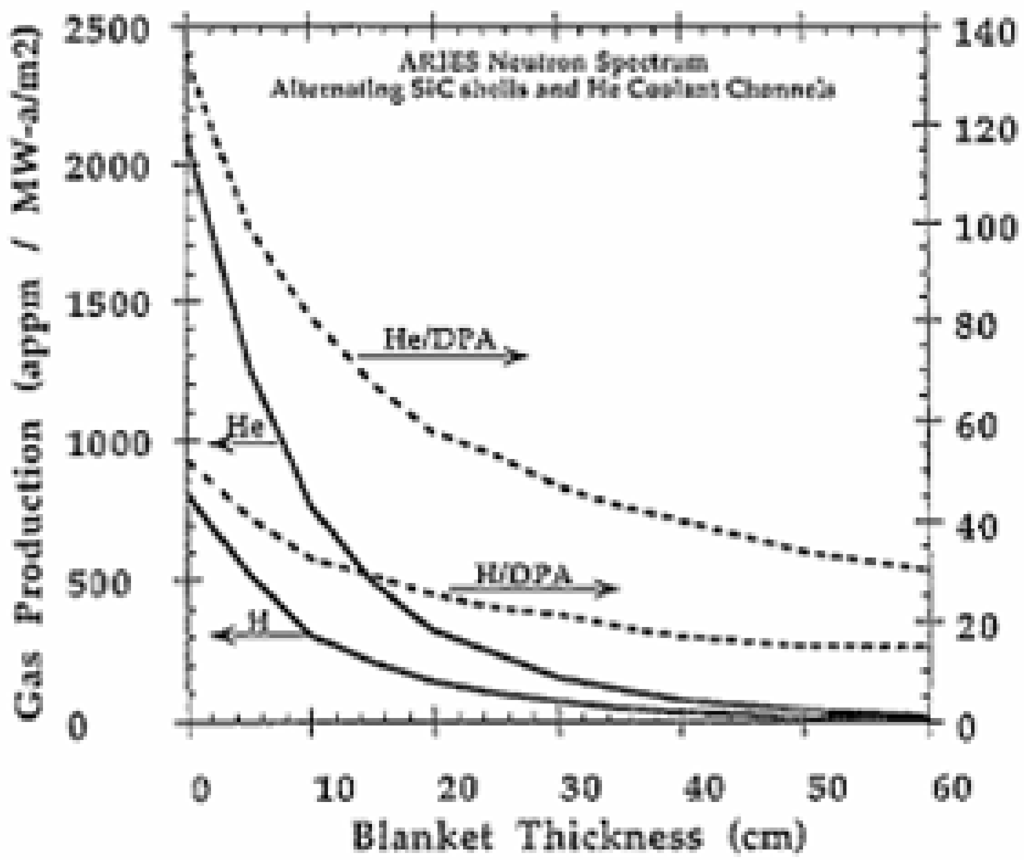

碳化矽複合材料中氦、氫原子產量與損傷程度的比例隨厚度變化關係圖

He = 150appm/dpa

H = 60appm/dpa

G.R. Hopkins, R.J. Price, Nucl. Eng. Des. 2(1984) 1

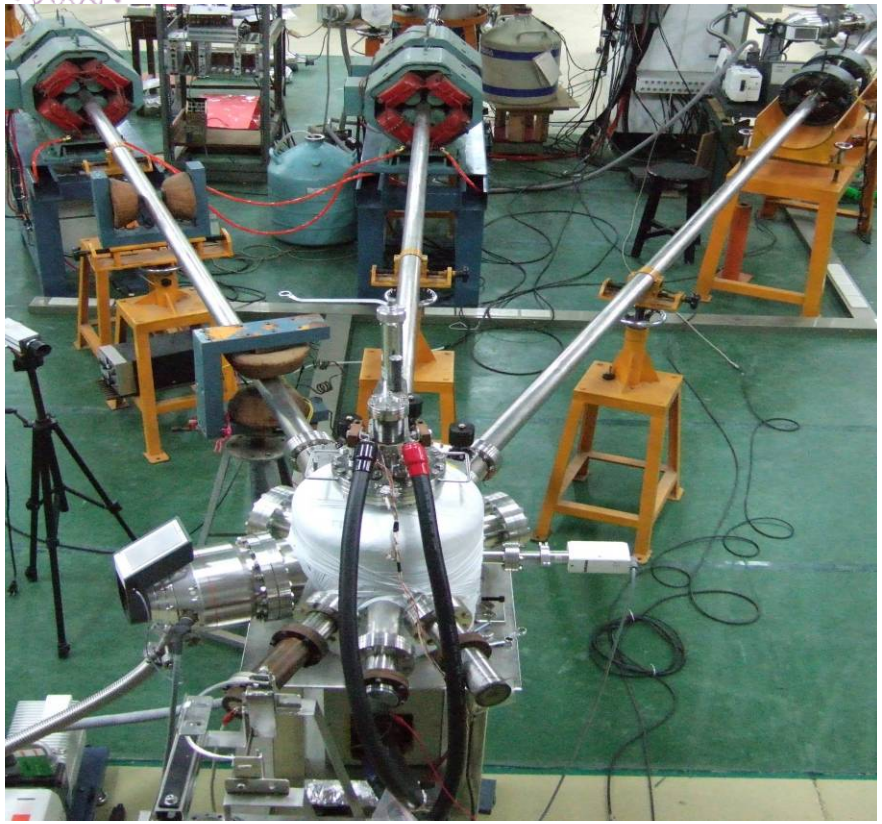

Triple beam ion implantation system

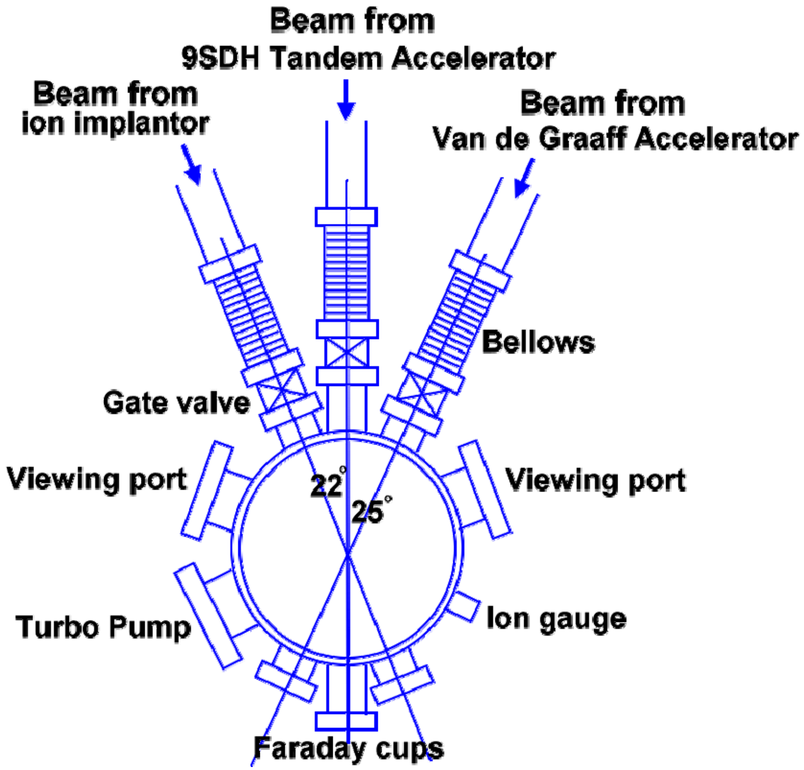

Triple beam implantation diagram

國立清華大學能源與環境研究中心
Center for Energy and Environmental Research

未照射未退火結構分析

- 由日本京都大學先進能源研究所製備Hi-Nicalon Type-S碳化矽纖維/碳/碳化矽

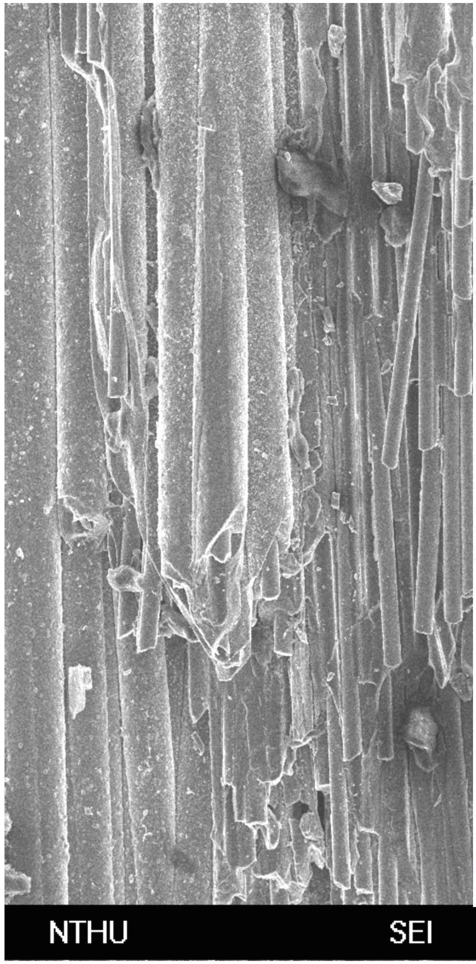

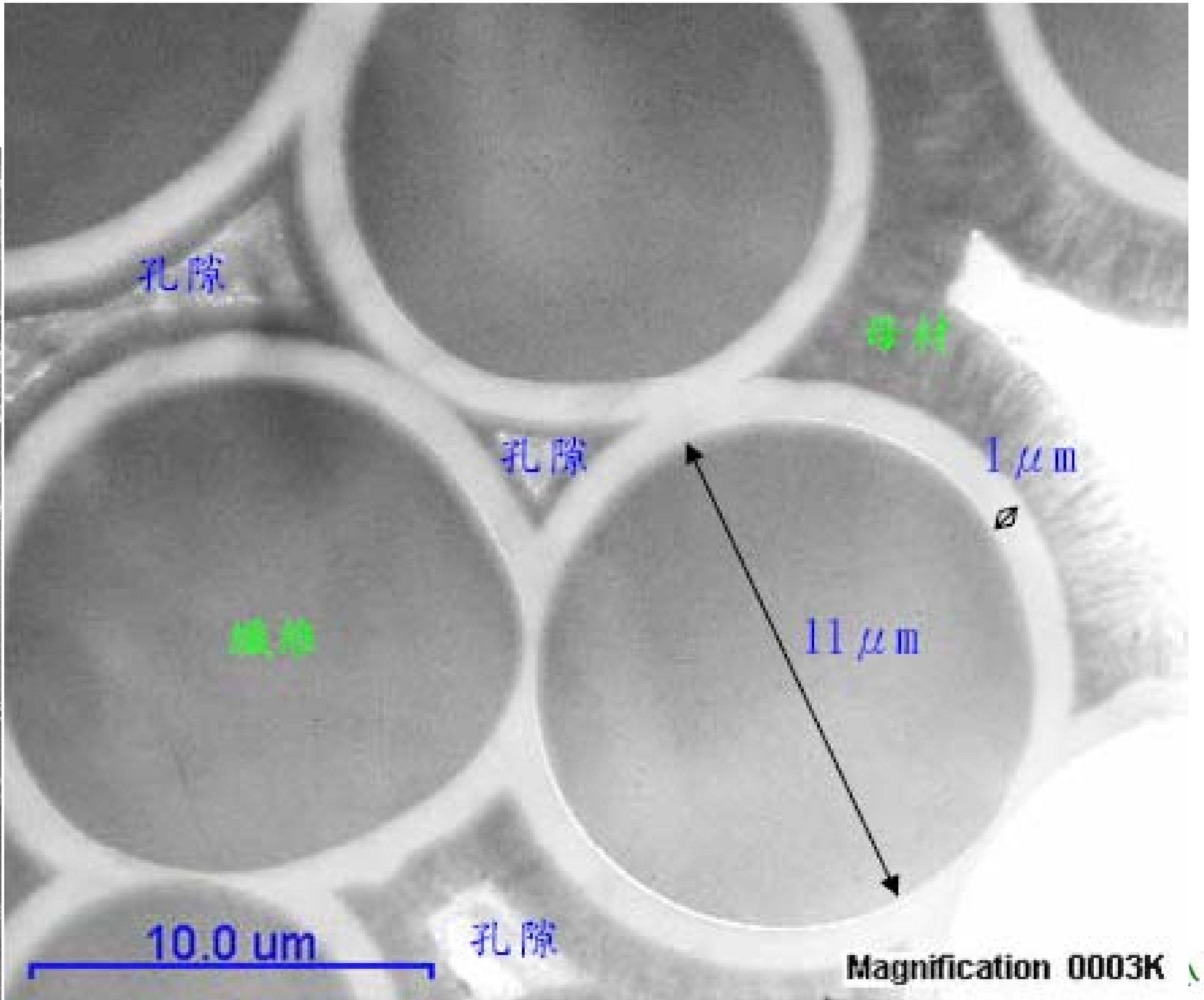

α碳化矽晶粒與β碳化矽晶粒

夾雜著3C、2H、4H、6H等結構的α碳化矽晶粒

純3C的

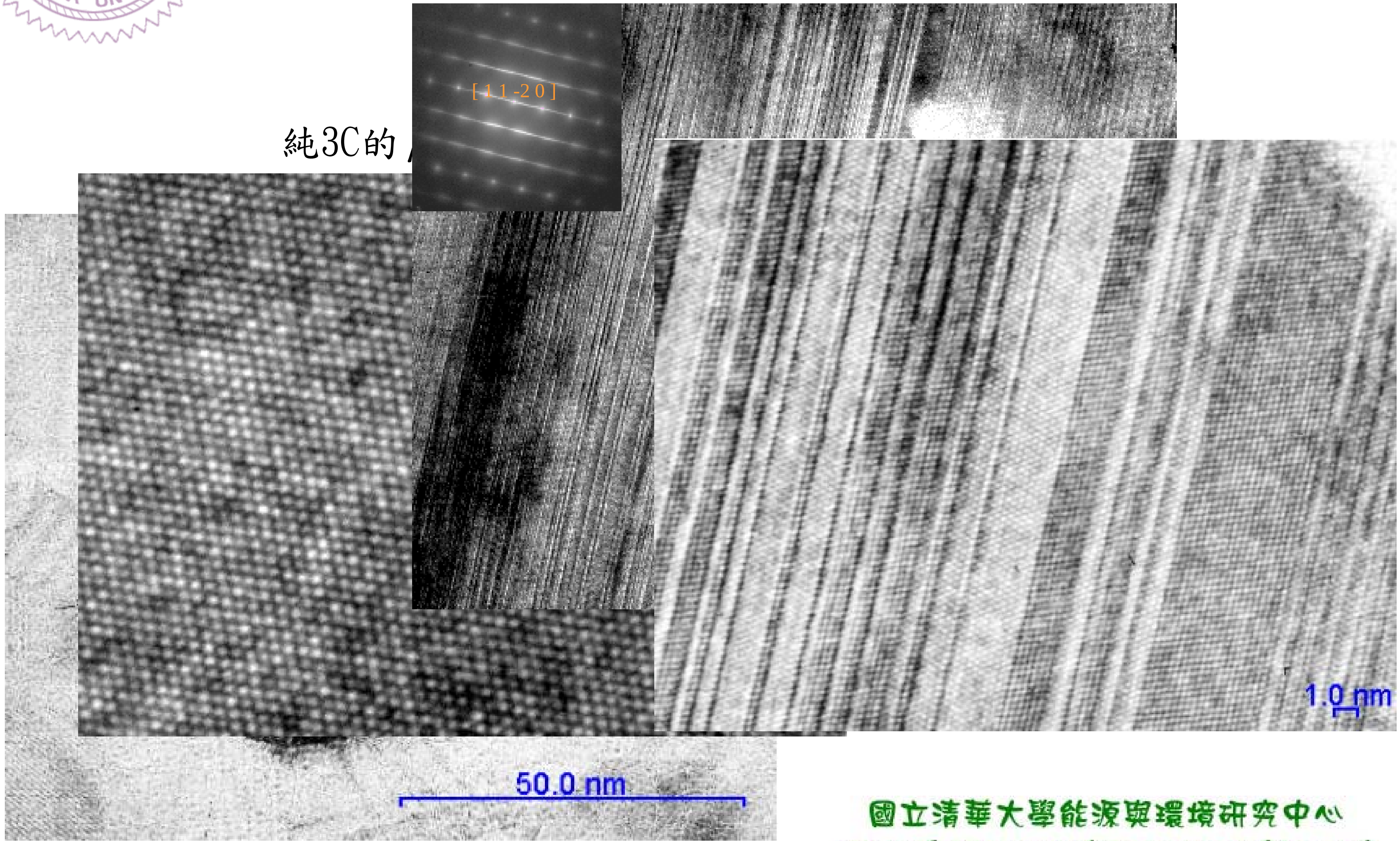

國立清華大學能源與環境研究中心
Center for Energy and Environmental Research

800°C 即時佈植氦、矽離子雙射束 (15000appm/100dpa)

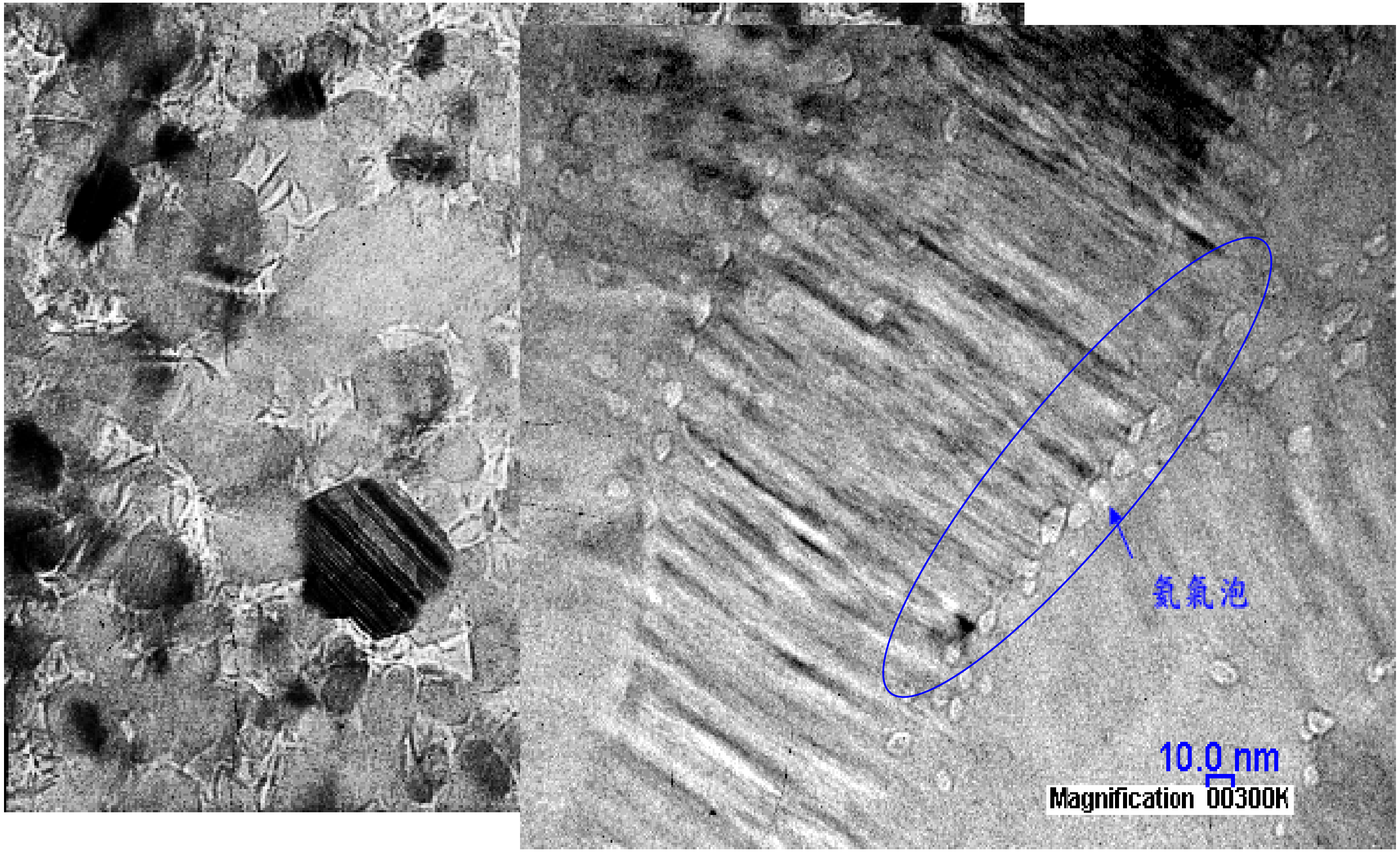

母材氦氣泡平均8.5nm；密度

1000°C 即時佈植氦、矽離子雙射束 (15000appm/100dpa)

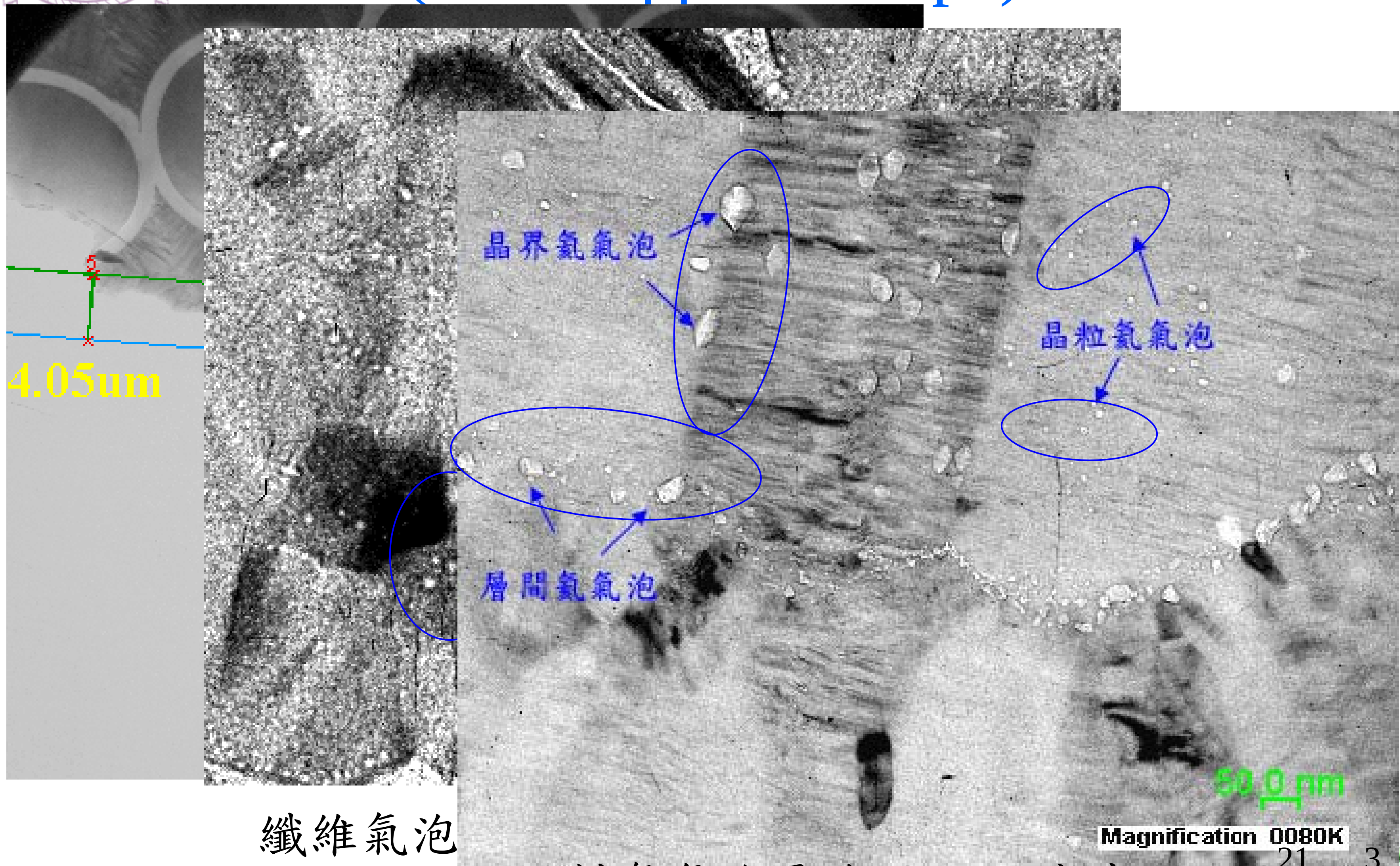

纖維氣泡

母材氦氣泡平均30nm；密度$5.7\times10^{21}/m^3$

Comparing the results of 800℃,1000℃ and 1200℃/high dose dual、triple-ion beams

He bubble / condition		SiC matrix (Swelling)		HNS SiC fiber	
		size(nm)	density(/m³)	size(nm)	density(/m³)
1#	800℃/100dpa/ 15000appm/6000appm	2.38±0.42	0.128%	X	X
2#	1000℃/100dpa/ 15000appm/6000appm	3.61±0.53 9.4±3.31	0.309%	1.98±0.28	1.62×10^{23}
3*	800℃/100dpa/ 15000appm	8.5±1.4	0.13%	X	X
4*	1000℃/100dpa/ 15000appm	30±7	1.77%	1.5±0.1	9.9×10^{21}
5@	1000℃/50dpa/ 65000appm/2000appm	15 4.5	Not mentioned	Not mentioned	Not mentioned
6	1200℃/80dpa/ 12000appm/4800appm	3.41±0.77 12.27±1.86	1.2%	1.78±0.41	7.97×10^{22}

Energy shifts of He K-edge are given with respect to the free atom value of 21.218eV

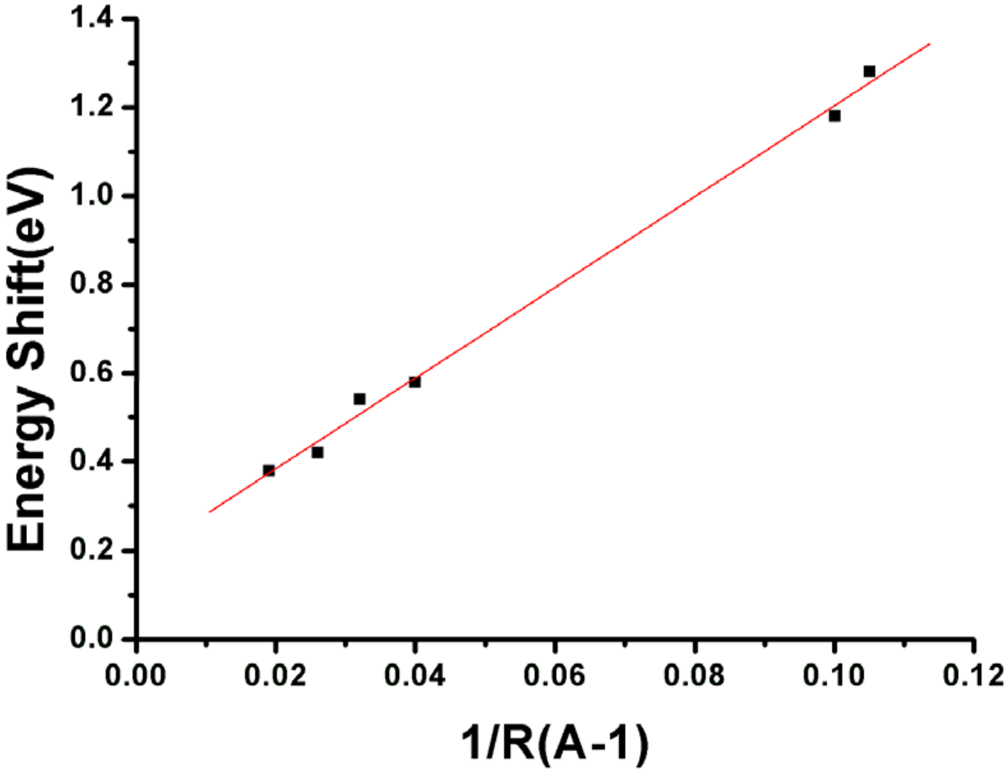

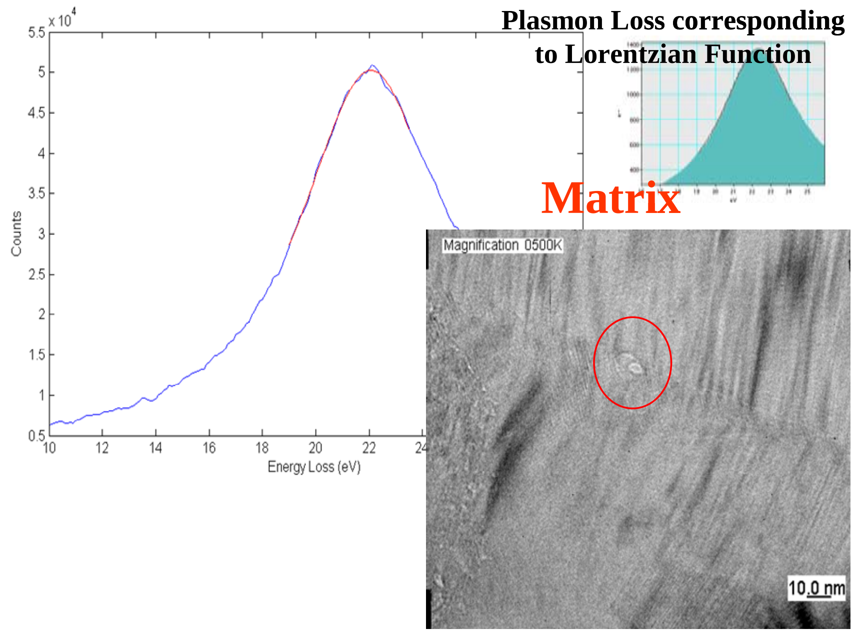

$$\Delta E(eV) = (0.18 \pm 0.02) + (10.26 \pm 0.32) \times (1/R(A))$$

Ion Implant Direction

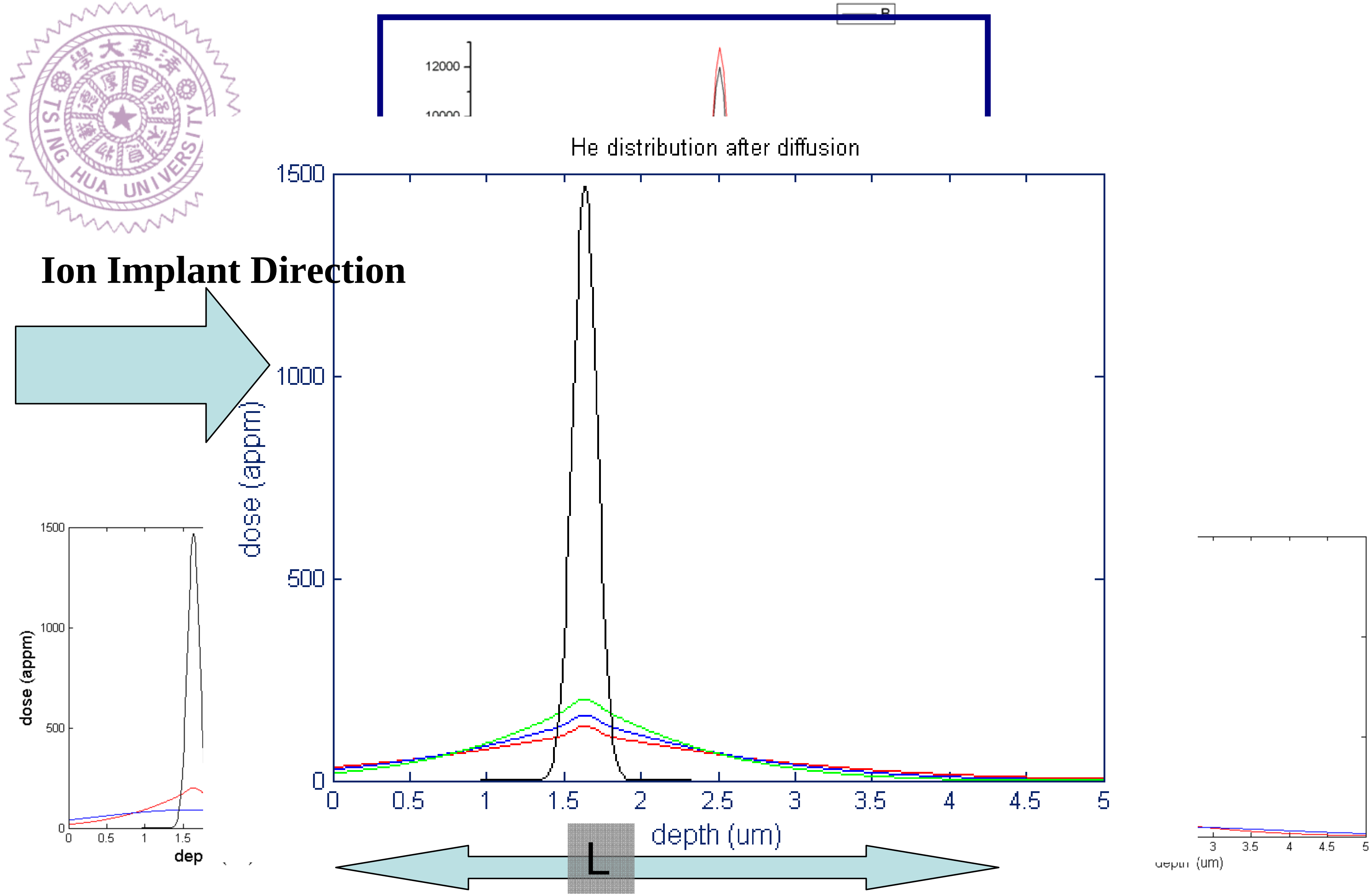

Simulation of He distribution at temperature range 1100°C to 1300°C

Incident dose of He: 2.97×10^{15} ions/cm^2

Ref. Journal of Nuclear Science and Technology, 41, 751

$$D(cm^2/s) = 1.38 \times 10^{-10} \exp[0.91(eV/atom)/kT]$$

$$\Delta E(eV) = (0.18 \pm 0.02) + (10.26 \pm 0.32) \times (1/R(A))$$

2r N N_0

10 dpa	Bubble Size (nm)	Bubble Density (1/m^3)	Energy Shift (eV)	He density (#/nm^3)	#/bubble	Helium Density (#/cm^3)	Implanting He density (#/cm^3)	He %
900°C/triple	2.16±0.29	6.19×10^{22}	1.13	41.3	218	1.35×10^{19}	**1.75×10^{19}**	**77.2%**
1000°C/triple	2.20±0.36	7.81×10^{22}	1.11	40.6	226	1.77×10^{19}	**1.24×10^{19}**	**100%**
1100°C/triple	2.38±0.43	3.1×10^{22}	1.0	38.5	272	8.42×10^{18}	**9.14×10^{18}**	**92.1%**
1200°C/triple	2.82±0.45	2.04×10^{22}	0.91	34.1	401	8.18×10^{18}	**8.49×10^{18}**	**96.3%**
1300°C/triple	2.32±0.32	2.10×10^{22}	1.06	39.2	256	5.38×10^{18}	**7.92×10^{18}**	**67.9%**

HTTR in JAEA Orari

HTTR

High Temperature Engineering Test Reactor

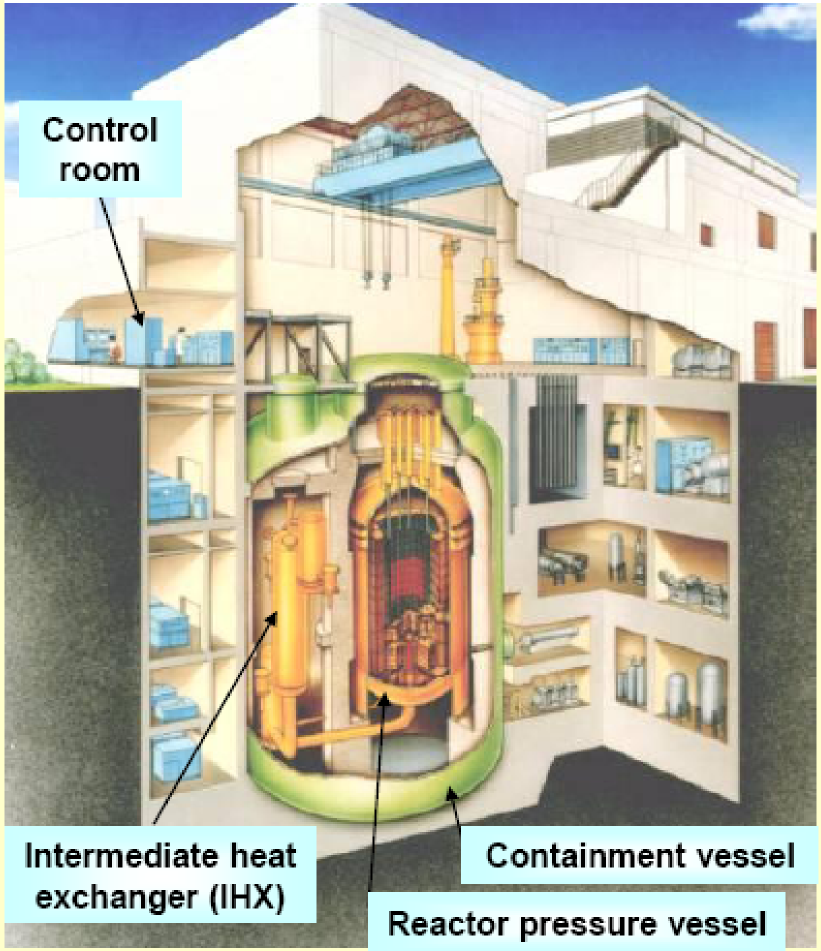

Main Objective

Establishment of HTGR technology

- Grasp HTGR operation performance
- Demonstration of inherent safety feature

Establishment of heat utilization technology

- Demonstration of hydrogen production system

Major specification

Thermal power	30 MW
Fuel	Coated fuel particle / Prismatic block type
Core material	Graphite
Coolant	Helium
Inlet temperature	395 °C
Outlet temperature	950 °C (Max.)
Pressure	4 MPa

3. HTTR facility (1/3) Fuel block

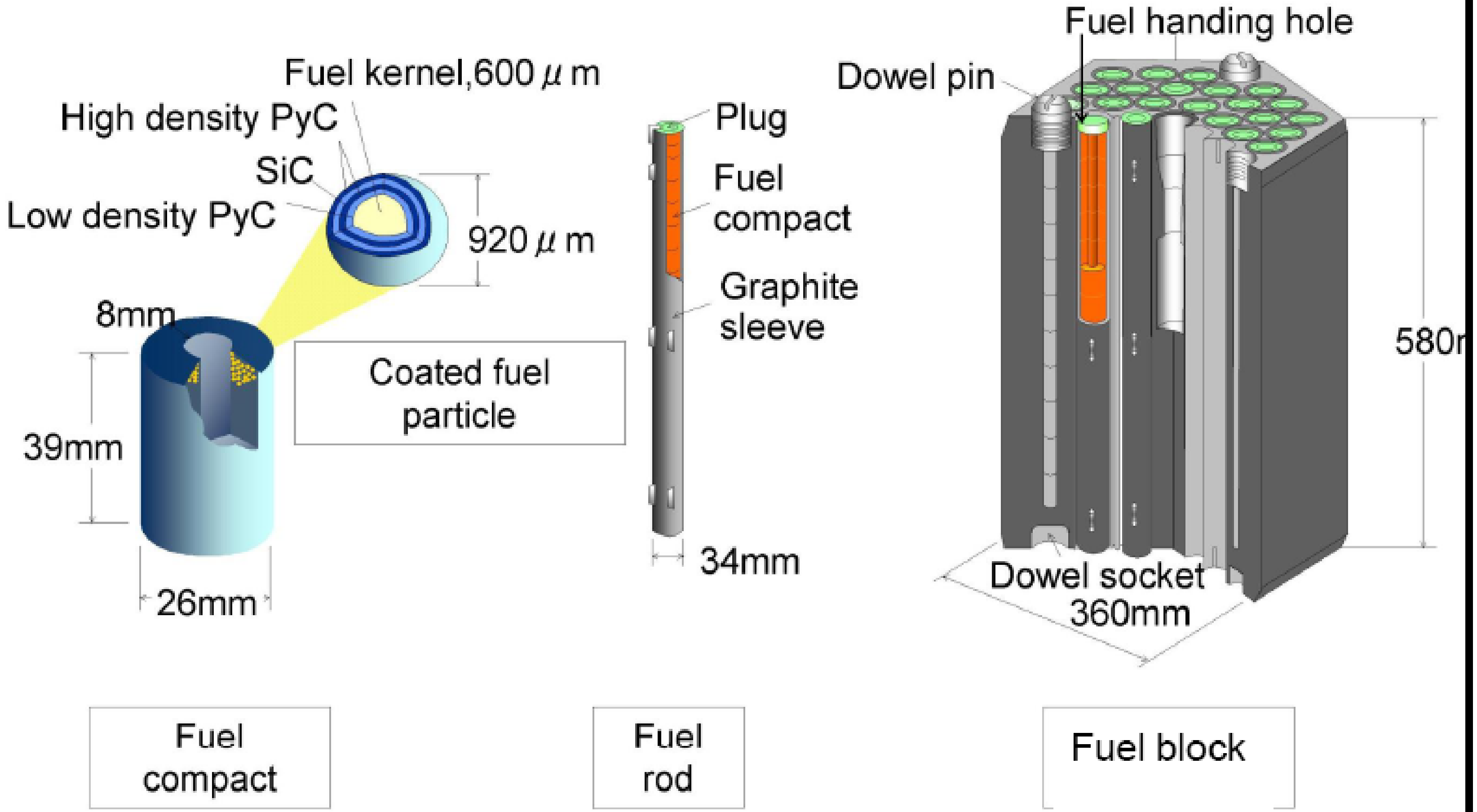

Materials and service conditions of HTTR high temperature components

Material		Components	Service conditions		Maximum allowable temperature
Material	Product form		Design temperature	Design pressure*	
2 1/4Cr-1Mo steel	Plate, forging, pipe	Reactor pressure vessel	440℃	4.8 MPa	550℃
		Shells of intermediate heat exchanger, primary pressurized water cooler, etc.	430℃	4.8 MPa	
		Outside pipe of concentric double pipe	430℃	4.8 MPa	
Hastelloy XR	Tube, plate, forging	Intermediate heat exchanger heat transfer tubes	955℃	0.29MPa	1000℃
		Intermediate heat exchanger hot header	940℃	0.29MPa	
SUS321	Tube	Primary pressurized water cooler heat transfer tubes	380℃	4.8 MPa	650℃
SUS316	Bar	Core restraint mechanism	450℃	-	650℃
1Cr-0.5Mo-V steel	Forging	Core restraint mechanism	450℃	-	450℃

*: absolute pressure,

Note: Control rod sleeves are made of Alloy 800H, whose maximum allowable temperature at a scram is 900℃.

Material and weld lines

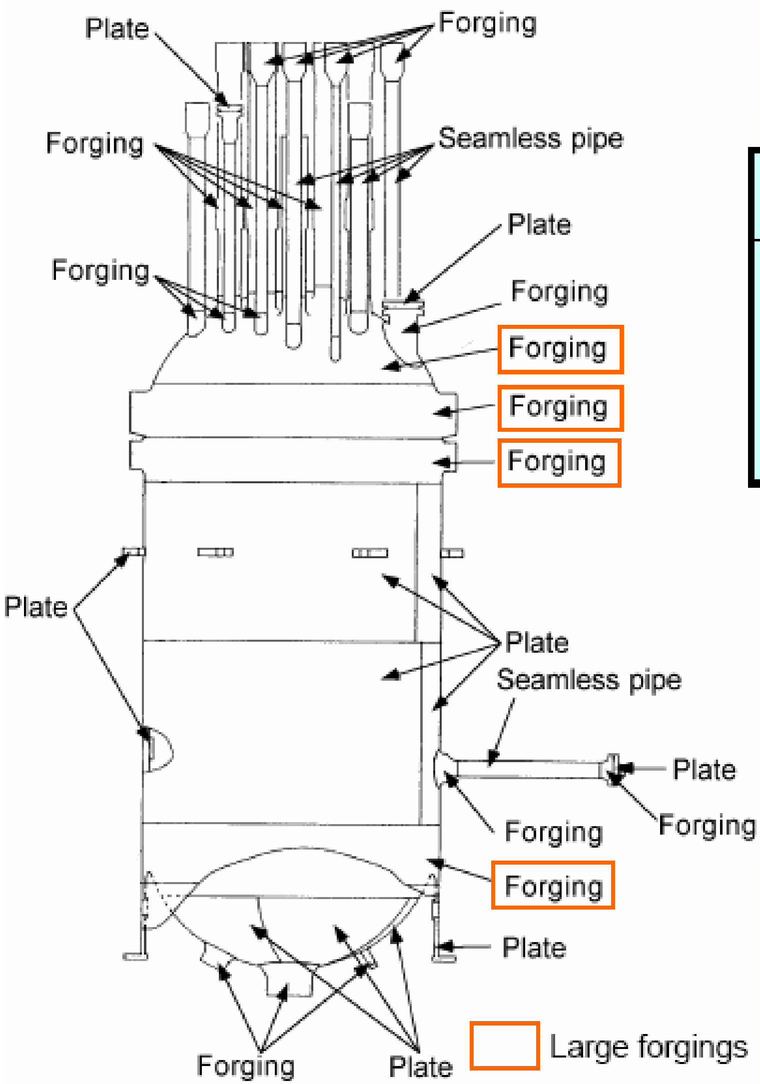

- 2 1/4Cr-1Mo steel (normalized and tempered)

Type	JIS	ASTM (equiv.)
Forging	SFVAF22B	A-336 Gr.F22, Cl.3
Plate	SCMV4-2	A-387 Gr.22, Cl.2
Pipe	STPA24	A-335 Gr.P22

- HTGR specification

J-factor = (Si+Mn)(P+Sn) $\times$104 $\leq$ 100
(Si, Mn, P, Sn : wt%)

$\overline{X}$=(10P+5Sb+4Sn+As)/100 $\leq$ 10
(P, Sb, Sn, As : ppm)

RT_{NDT} (Reference Temperature) $\leq$ -20 °C

Effect of neutron fluence on the change in $_vT_{r41J}$

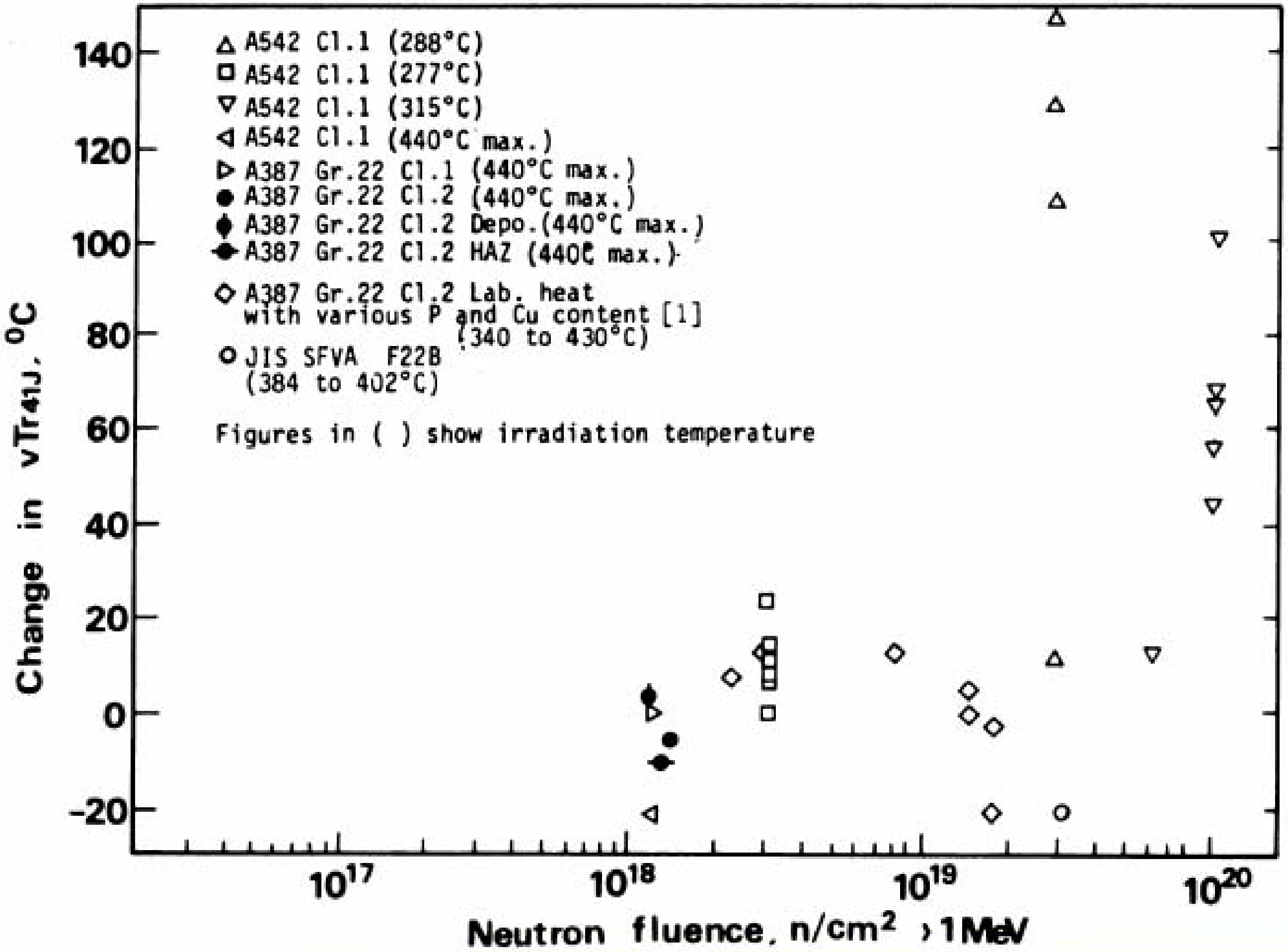

Radiation Damage in Nuclear Grade Graphite in Simulated VHTGR Core Environment

Determination of d_c from HRTEM images

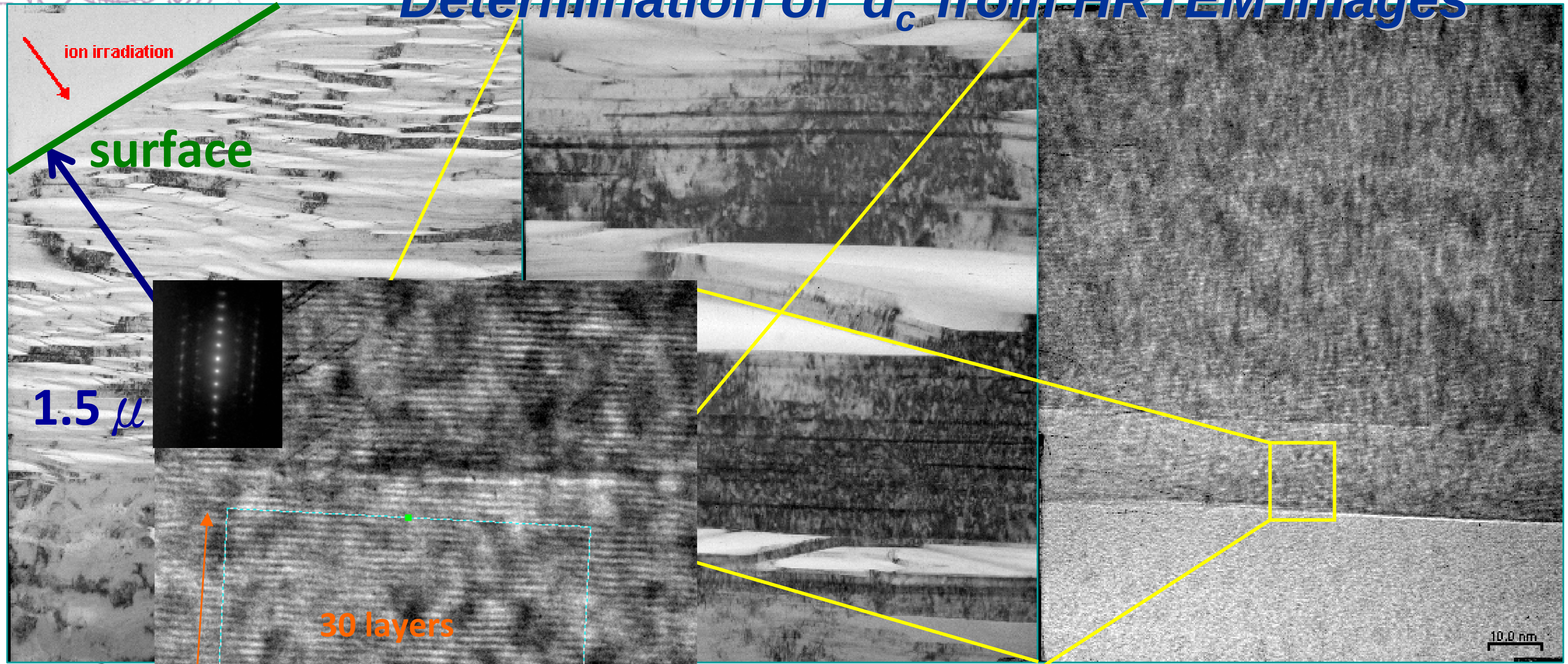

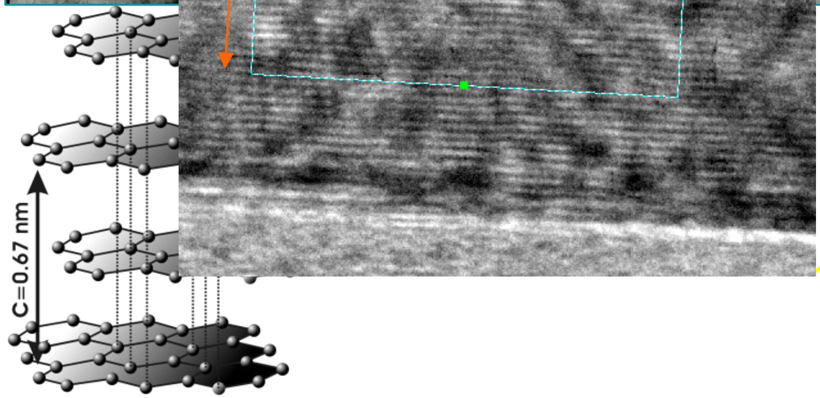

Graphite was irradiated at 600℃
Depth: 1.5 μm
Dose: 0.6dpa

國立清華大學能源與環境研究中心
Center for Energy and Environmental Research

HRTEM images from the region of different doses

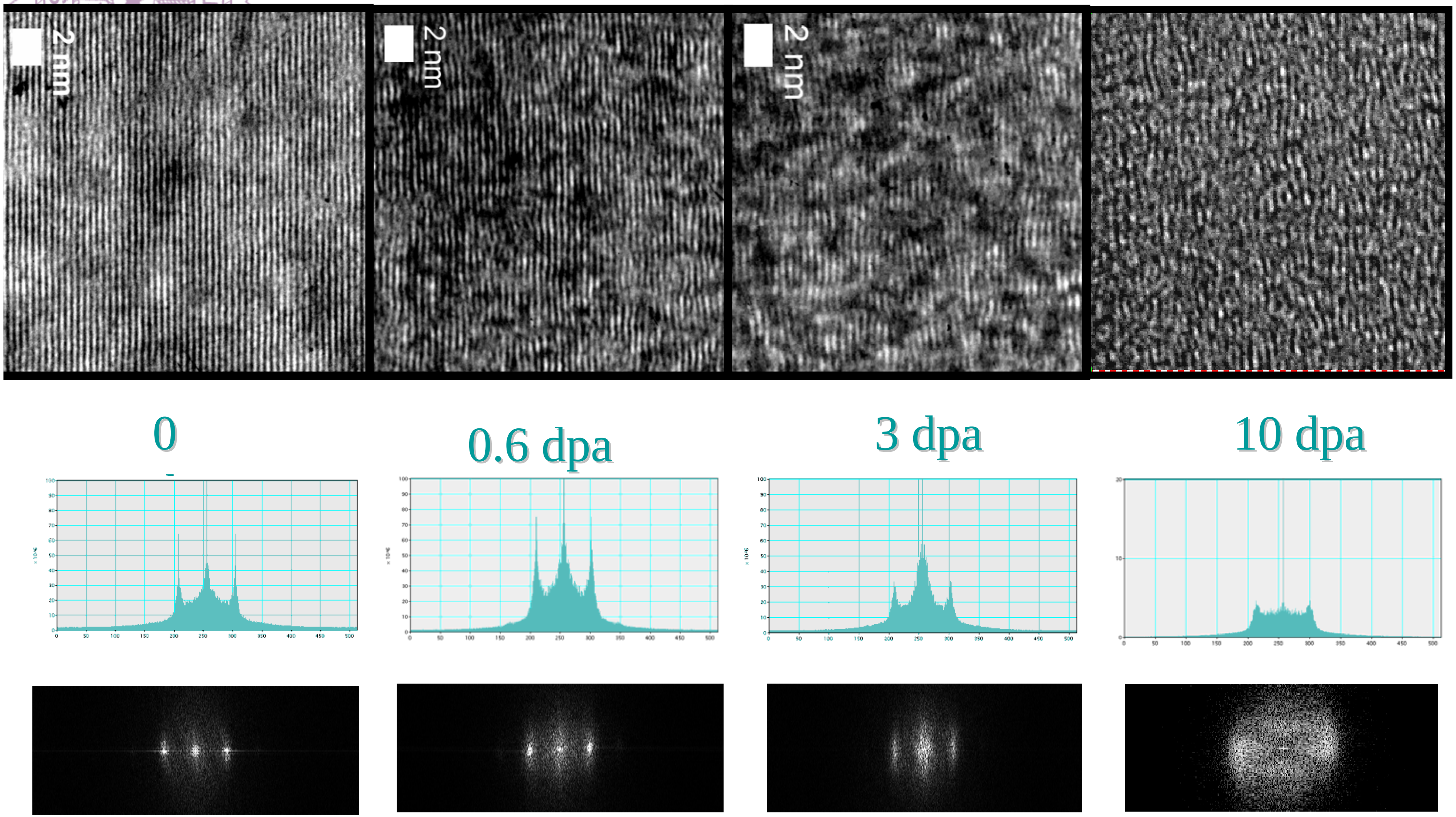

Calculation of storage energy in nuclear grade graphite

				only c- axis		a+c axis	
	dose(dpa)	d spacing(nm)	strain of c spacing(%)	strain energy(cal/g)	rising temperature(℃)	strain energy(cal/g)	rising temperature(℃)
500	0.6	0.344±0.002	2.4	40±4	105±11	81±9	215±22
	3	0.355±0.002	5.7	222±24	536±55	518±52	1368±128
	5	0.361±0.003	7.6	279±20	735±54	847±59	2087±146
	10	0.381±0.007	13.5	791±47	2087±123	2681±158	7073±417
600	0.6	0.358±0.002	6.7	108±11	264±27	397±38	1008±93
	3	0.362±0.002	7.7	289±28	670±66	793±83	2014±223
	5	0.372±0.004	10.8	308±11	783±26	1057±38	3465±126
	10	0.396 ±0.011	17.8	764 ±118	1939 ±299	3624 ±558	9197 ±1416
700	0.6	0.357±0.002	6.3	83±8	199±20	316±33	777±79
	3	0.359±0.002	7	209±19	483±47	584±59	1434±145
	5	0.365±0.003	8.6	249±21	612±53	845±73	2076±176
	10	0.389±0.01	16.1	691± 76	1697± 187	2828±311	6947±764
800	0.6	0.355±0.002	5.8	63±8	160±18	263±30	630±65
	3	0.357±0.003	6.3	160±18	366±39	447±42	1069±96
	5	0.363±0.004	8.1	199±21	475±50	694±74	1661±176
	10	0.382±0.006	13.6	617±94	1475±226	2125±330	5166±790

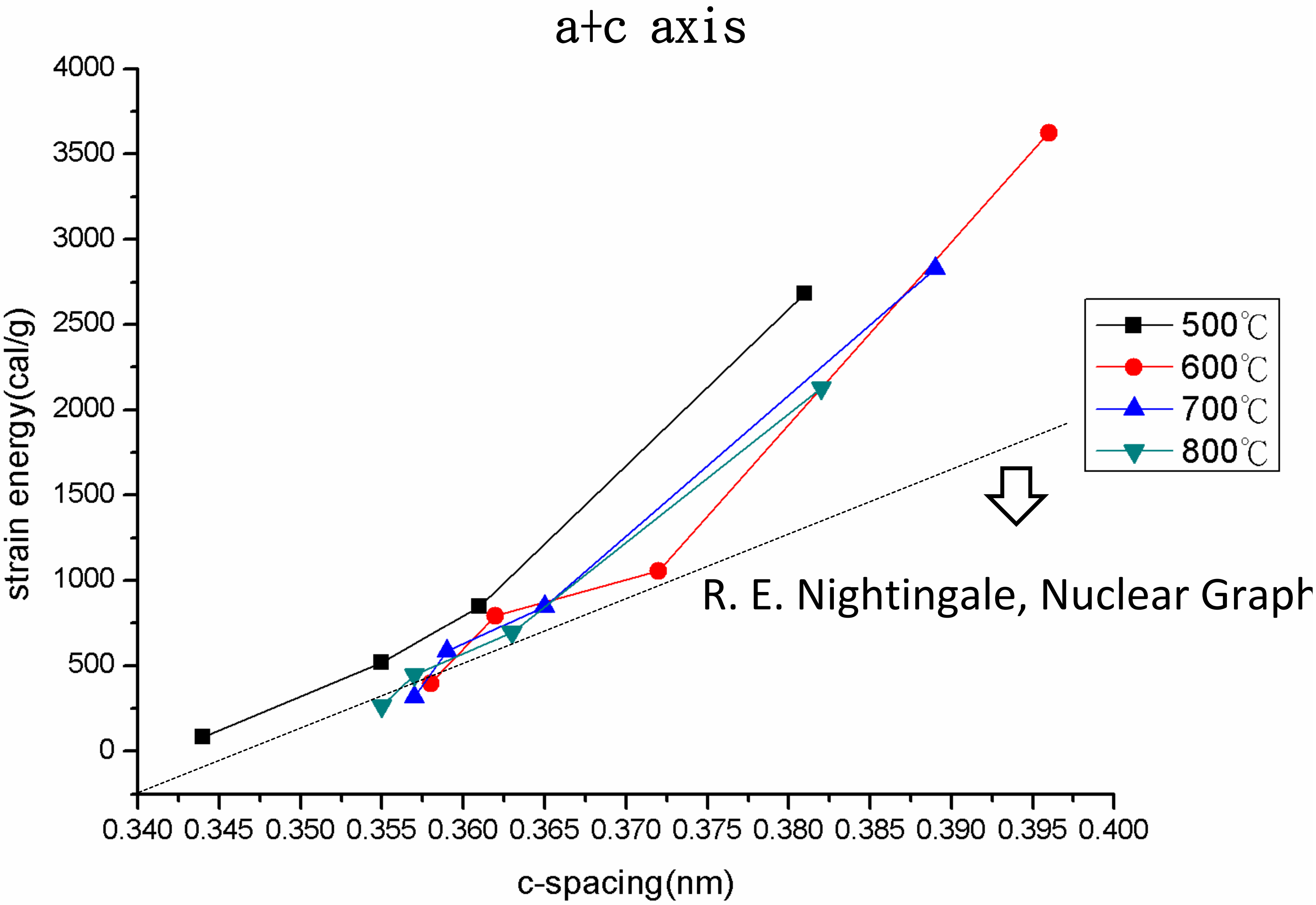

Strain energy changes due to different c-spacing(c+a -axis)

High-temperature corrosion of Inconel 625 in supercritical water

Mass change

Compared with $w^n=kt$ ，$n=2.21$，$k=1.4\times10^{-5}$ $mg^2/cm^4/hour$，n is approach to 2，It matched the parabolic curve .

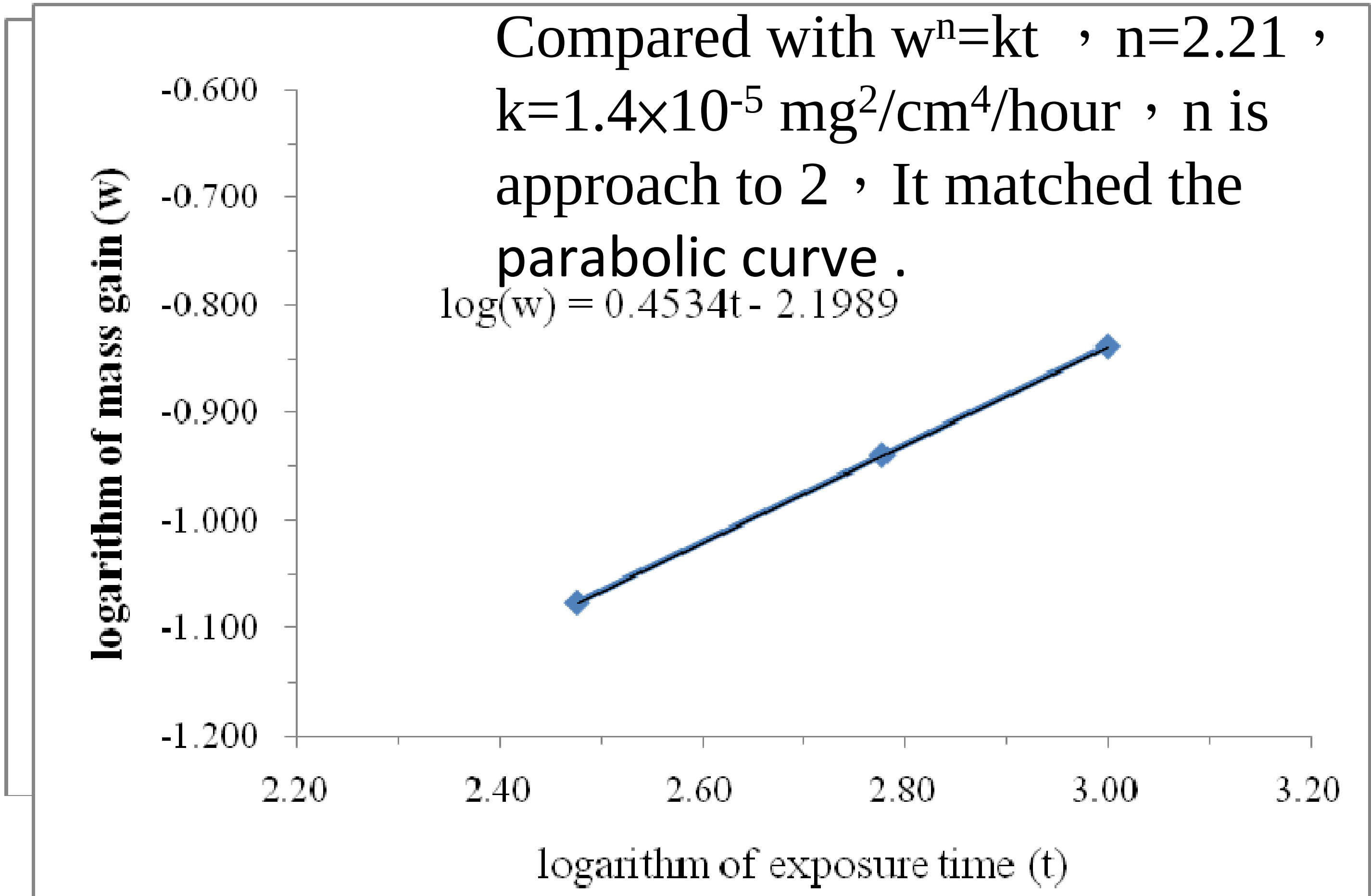

Cross-section Investigation for TEM

The EDX analysis and the electron diffraction patterns of the oxide layer for Inconel 625 after exposed to 8.3 ppm D.O. SCW at 600°C for 600h.

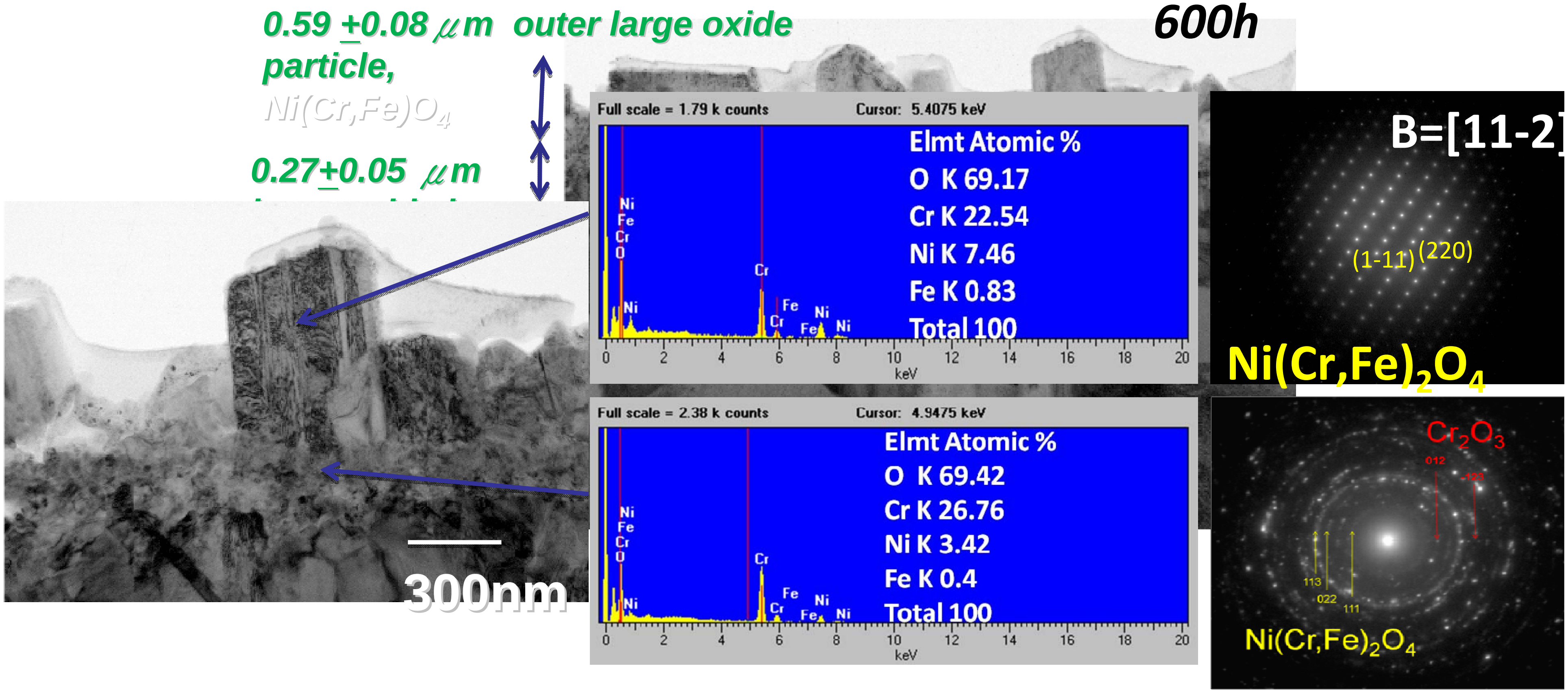

國立清華大學能源與環境研究中心
Center for Energy and Environmental Research

Radiation Effect

Ni^{2+} implanted on Inconel 625 at 600°C to 15 dpa

Dislocation density = $1.2X10^{21}$ m^{-3}
Dislocation density of as-received Inconel 625 =$1.2X10^{20}$$m^{-3}$

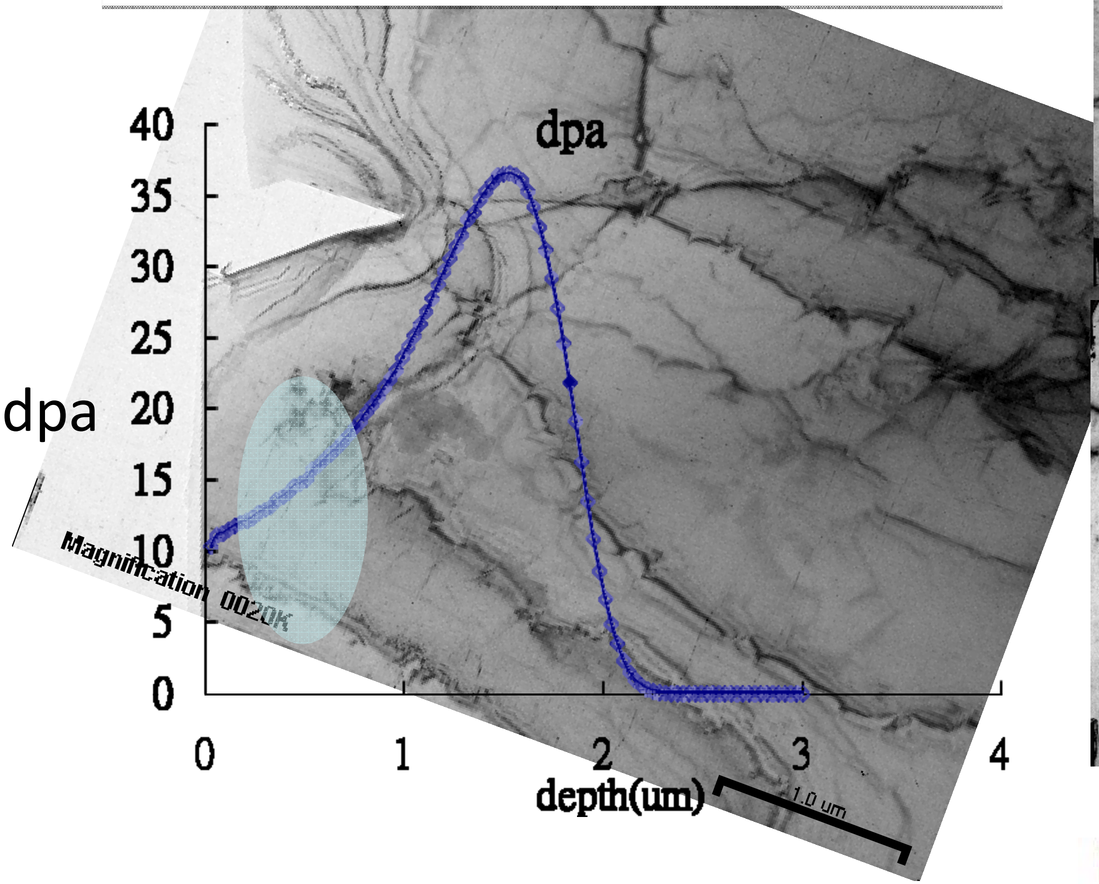

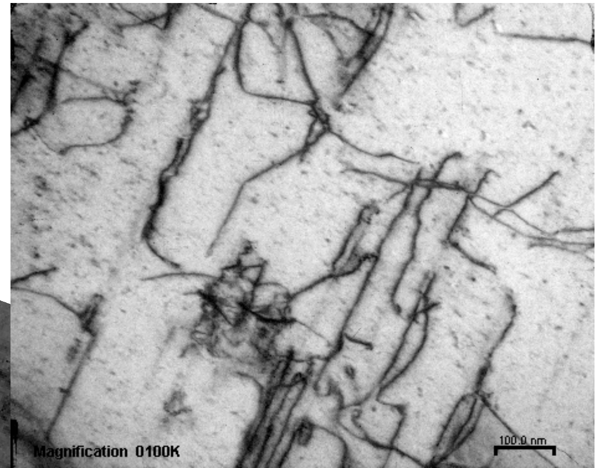

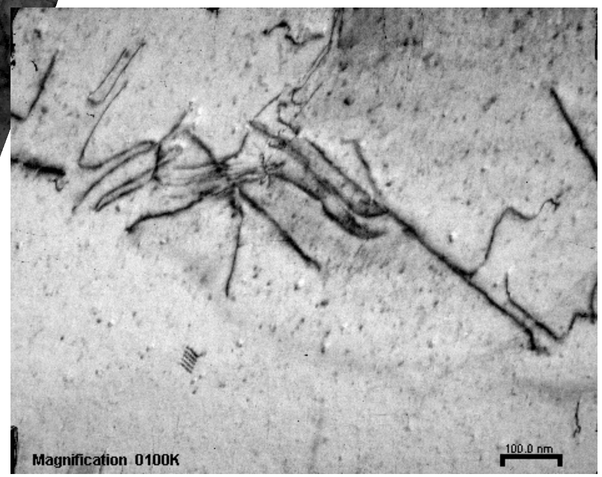


Department of Engineering and System Science
Thank you !!
DEC 1 2005